

# Towards an algebraic method of solar cycle prediction

## II. Reducing the need for detailed input data with *ARDoR*

Melinda Nagy<sup>1</sup>, Kristóf Petrovay<sup>1</sup>, Alexandre Lemerle<sup>2,3</sup>, and Paul Charbonneau<sup>2</sup>

<sup>1</sup> Eötvös Loránd University, Department of Astronomy, Budapest, Hungary  
e-mail: [M.Nagy@astro.elte.hu](mailto:M.Nagy@astro.elte.hu), [K.Petrovay@astro.elte.hu](mailto:K.Petrovay@astro.elte.hu)

<sup>2</sup> Département de Physique, Université de Montréal, Montréal, QC, Canada  
e-mail: [paulchar@astro.umontreal.ca](mailto:paulchar@astro.umontreal.ca), [lemerle@astro.umontreal.ca](mailto:lemerle@astro.umontreal.ca)

<sup>3</sup> Bois-de-Boulogne College, Montréal, QC, Canada

### ABSTRACT

An algebraic method for the reconstruction and potentially prediction of the solar dipole moment value at sunspot minimum (known to be a good predictor of the amplitude of the next solar cycle) was suggested in the first paper in this series. The method sums up the ultimate dipole moment contributions of individual active regions in a solar cycle: for this, detailed and reliable input data would in principle be needed for thousands of active regions in a solar cycle. To reduce the need for detailed input data, here we propose a new active region descriptor called *ARDoR* (Active Region Degree of Rogueness). In a detailed statistical analysis of a large number of activity cycles simulated with the  $2 \times 2D$  dynamo model we demonstrate that ranking active regions by decreasing *ARDoR*, for a good reproduction of the solar dipole moment at the end of the cycle it is sufficient to consider the top  $N$  regions on this list explicitly, where  $N$  is a relatively low number, while for the other regions the *ARDoR* value may be set to zero. E.g., with  $N = 5$  the fraction of cycles where the dipole moment is reproduced with an error exceeding  $\pm 30\%$  is only 12%, significantly reduced with respect to the case  $N = 0$ , i.e. *ARDoR* set to zero for all active regions, where this fraction is 26%. This indicates that stochastic effects on the intercycle variations of solar activity are dominated by the effect of a low number of large “rogue” active regions, rather than the combined effect of numerous small ARs. The method has a potential for future use in solar cycle prediction.

**Key words.** solar cycle – cycle prediction – rogue sunspots – surface flux transport modeling

## 1. General introduction

The magnetic fields responsible for solar activity phenomena emerge into the solar atmosphere in a concentrated form, in active regions (ARs). In each solar cycle thousands of active regions are listed in the official NOAA database and many more small active regions are missed if their heliographic position and lifetime do not render them directly observable on the visible hemisphere. Similarly, no detailed catalogues exist for the ubiquitous ephemeral active regions, of even smaller size.

The emergence of this large number of (typically) bipolar magnetic regions obeys some well known statistical regularities like Hale’s polarity rules and Joy’s law. As a consequence, upon their decay by turbulent diffusion their remains contribute to the large-scale ordered photospheric magnetic field, including the Sun’s global axial dipole field (the so-called Babcock–Leighton mechanism). Active regions emerging in a given solar cycle contribute on average to the global dipole with a sign opposite to the preexisting field at the start of the cycle, and these contributions from active regions add up until, some time in the middle of the cycle, the global field reverses and a new cycle starts at the Sun’s poles, still overlapping with the ongoing cycle at low latitudes. Flux emergence is thus an important element of the solar dynamo mechanism sustaining the periodically overturning solar magnetic field.

The inherently stochastic nature of flux emergence introduces random fluctuations into this statistically ordered process. In recent years it has been realized that the random nature of flux emergence can give rise to significant deviations of the solar dipole moment built up during a cycle from its expected mean value: in some cycles a small number of so-called “rogue” active regions (Petrovay and Nagy 2018) with atypical properties may lead to a major, unexpected change in the level of activity. The unexpected change in the level of activity from solar cycle 23 to 24 has been interpreted as the result a few such abnormal regions by Jiang et al. [2015], while in a dynamo model Nagy et al. [2017] found that in extreme cases even a single rogue AR can trigger a grand minimum.

An open question is how to identify the [candidate] rogue active regions, and how many such regions need to be considered in individual detail in models aiming to reproduce the evolution of the Sun’s large scale field. It is not a priori clear that this number is low, so the question we pose in this paper is whether the stochastic effects in cycle-to-cycle variation originating in the random nature of the flux emergence process are dominated by a few “rogue” AR in each cycle with individually large and unusual contributions to the dipole moment, or by the “fluctuation background” due to numerous other AR with individually much lower deviations from the expected dipole contribution. While the recent studies cited above stressed the importance of a few large rogue AR, the importance of the fluctuation background cannot be discarded out of hand. The issue has obvious practical significance from the point of view of solar cycle prediction: it would be useful to know how many (and exactly which) observed individual AR need to be assimilated into a model for successful forecasts.

A related investigation was recently carried out by Whitbread et al. [2018]. In that work ARs were ordered by their individual contributions to the global axial dipole moment: it was found that, far from being dominated by a few ARs with the largest contributions, the global dipole moment built up during a cycle cannot be reproduced without taking into account

73 a large number (hundreds) of ARs. In another recent work [Cameron and Schüssler \[2020\]](#)  
 74 found that even ephemeral active regions contribute to the net toroidal flux loss from the  
 75 Sun by an amount comparable to the contribution of large active regions. By analogy, this  
 76 opens the possibility that ephemeral ARs may also contribute to the global poloidal field by  
 77 a non-negligible amount, though statistical studies of the orientation of ephemeral ARs are  
 78 unfortunately rare (cf. [Tlatov et al. 2010](#)).

79 While these interesting results shed new light on the overall role of flux emergence in smaller  
 80 bipoles in the global dynamo, we think that from the point of view of solar cycle prediction,  
 81 instead of the dipole moment contribution per se, a more relevant control parameter is the  
 82 *deviation* of the dipole contribution from the case with no random fluctuations in flux emer-  
 83 gence, i.e. the “degree of rogueness” (DoR). We therefore set out to systematically study  
 84 the effect of individual AR on the subsequent course of solar activity using the DoR as an  
 85 ordering parameter.

86 The question immediately arises how this DoR should be defined.

87 The approach we take in this work assumes that the effect of random fluctuations manifests  
 88 itself primarily in the properties of individual active regions, rather than in their spatiotem-  
 89 poral distribution. The DoR based on individual AR properties will be called “active region  
 90 degree of rogueness” — *ARDoR* for brevity.

91 The structure of this paper is as follows. Section 2 introduces and discusses our definition  
 92 of *ARDoR*. In Section 3, after recalling salient features of the  $2 \times 2D$  dynamo model, we use  
 93 statistics based on this model to answer the central question of this paper. Conclusions are  
 94 drawn in Section 4.

## 95 2. Introducing *ARDoR*

96 The Sun’s axial dipolar moment is expressed as

$$97 \quad D(t) = \frac{3}{2} \int_{-\pi/2}^{\pi/2} B(\lambda, t) \sin \lambda \cos \lambda \, d\lambda, \quad (1)$$

98 where  $B$  is the azimuthal average of the large scale photospheric magnetic field (assumed to  
 99 be radial) while  $\lambda$  is heliographic latitude.

100 The value  $D_n$  of this dipole moment at the start of cycle  $n$  is widely considered the  
 101 best physics-based precursor of the the amplitude of the incipient cycle  $n$  ([Petrovay 2020](#)).  
 102 Understanding intercycle variations in solar activity and potentially extending the scope of  
 103 the prediction calls for an effective and robust method to compute  $D_n$  from (often limited)  
 104 observational data on the previous course of solar activity.

105 In the first paper of this series, [Petrovay et al. \[2020\]](#) (hereafter Paper 1) we suggested a  
 106 simplified approach to the computation of the evolution of the global axial dipole moment  
 107 of the Sun. Instead of solving the partial differential equation normally used for modeling  
 108 surface magnetic flux transport (SFT) processes on the Sun, this method simply represents  
 109 the dipole moment by an algebraic sum:

$$110 \quad \Delta D_n \equiv D_{n+1} - D_n = \sum_{i=1}^{N_{\text{tot}}} \delta D_{U,i} = \sum_{i=1}^{N_{\text{tot}}} \delta D_{\infty,i} e^{(t_i - t_{n+1})/\tau} = \sum_{i=1}^{N_{\text{tot}}} f_{\infty,i} \delta D_{1,i} e^{(t_i - t_{n+1})/\tau}, \quad (2)$$

111 where  $i$  indexes the active regions in a cycle,  $N_{\text{tot}}$  is the total number of ARs in the cycle,  
 112  $\delta D_1$  is the *initial* contribution of an active region to the global dipole moment,  $\delta D_U$  is its  
 113 *ultimate* contribution at the end of a cycle and  $\tau \leq \infty$  is the assumed timescale of magnetic  
 114 field decay due to radial diffusion. Furthermore,

$$115 \quad f_\infty = \delta D_\infty / \delta D_1, \quad (3)$$

116 where  $\delta D_\infty$  is the *asymptotic* contribution of the same AR in a SFT model with  $\tau = \infty$ , once  
 117 the meridional flow has concentrated the relic magnetic flux from the AR to two opposite  
 118 polarity patches at the two poles. (See Paper 1 for further explanations.)

119 In this approach, ARs are assumed to be represented by simple bipoles at the time of their  
 120 introduction into the model so their initial dipole moment contribution is given by

$$121 \quad \delta D_1 = \frac{3}{4\pi R^2} \Phi d_\lambda \cos \lambda_0, \quad (4)$$

122 where  $\Phi$  is the magnetic flux in the northern polarity patch,  $d_\lambda$  is the latitudinal separation  
 123 of the polarities<sup>1</sup>,  $\lambda_0$  is the initial latitude of [the center of] the bipole and  $R$  is the radius of  
 124 the Sun. As demonstrated in Paper 1,  $f_\infty$ , is in turn given by

$$125 \quad f_\infty = \frac{a}{\lambda_R} \exp\left(\frac{-\lambda_0^2}{2\lambda_R^2}\right). \quad (5)$$

126 It was numerically demonstrated in Paper 1 that this Gaussian form holds quite generally  
 127 irrespective of the details of the SFT model, its parameters ( $\lambda_R$  and  $a$ ) only have a very  
 128 weak dependence on the assumed form of the meridional flow profile (at least for profiles  
 129 that are closer to observations), and their value only depends on a single combination of SFT  
 130 model parameters. The values of  $\lambda_R$  and  $a$  for a given SFT model may be determined by  
 131 interpolation of the numerical results, as presented in Paper 1.

132 The terms of the sum (2) represent the ultimate dipole contributions  $\delta D_U$  of individual  
 133 active regions in a cycle at the solar minimum ending that cycle. In principle each and every  
 134 active region should be represented by an explicit term in the sum. Such a case was indeed  
 135 considered in Paper 1 in a comparison with a run result from the 2×2D dynamo and it was  
 136 found that the algebraic method returns the total change in dipole moment during a cycle  
 137 quite accurately in the overwhelming majority of cycles.

138 When it comes to applying the method to the real Sun, however, the need to include each  
 139 bipolar region in the source becomes quite a nuisance. As discussed above in the Introduction,  
 140 data for individual active regions are often missing for the smaller ARs, while in the case of  
 141 the larger, more complex AR representing them by an instantaneously introduced bipole is  
 142 nontrivial. As it was recently pointed out by Iijima et al. [2019], for an AR with zero tilt but  
 143 different extents of the two polarity distributions  $\delta D_\infty$  will be nonzero, even though  $\delta D_1 = 0$   
 144 for this configuration. The reason is that the configuration has a nonzero quadrupole moment,  
 145 which may alternatively be represented by not one but two oppositely oriented dipoles slightly  
 146 shifted in latitude.

---

<sup>1</sup>  $d_\lambda = d \sin \alpha$  where  $d$  is the full angular polarity separation on the solar surface and  $\alpha$  is the tilt  
 angle of the bipole axis relative to the east–west direction, the sign of  $\alpha$  being negative for bipoles  
 disobeying Hale’s polarity rules.

Such intricacies would certainly make it advisable to keep the number of active regions explicitly represented in the sum (2) to a minimum. This again brings us to the central question of this paper: how many and which active regions need to be explicitly taken into consideration for the calculation of the solar dipole moment? While the previous study of Whitbread et al. [2018] has shown that keeping only a few ARs in the summation is certainly not correct, representing the rest of the ARs in a less faithful or detailed manner may still be admissible as long as this does not distort the statistics.

To select those few ARs that still need to be realistically represented we introduce the concept of *ARDoR*. As known examples of rogue AR presented e.g. in Nagy et al. (2017) are primarily rogue on account of their unusual tilts and large separations, the first idea is to define *ARDoR* as the difference between the ultimate dipole moment contribution of an AR and the value this would take with no scatter in the tilt and separation (i.e. if the tilt and separation were to take their expected values for the given latitude and magnetic flux, as given by eqs. (15) and (16a) in Lemerle et al. 2015).

In the present paper we thus consider the case where for the majority of ARs only the information regarding their size (magnetic flux) and heliographic latitude is retained, while further details such as polarity separation or tilt angle (and therefore  $\delta D_1$ ) are simply set to their expected values for the ARs with the given flux and heliographic latitude (“reduced stochasticity” or RS representation), and compare this with the case when the actual polarity separations and tilts are used (“fully stochastic” or FS case). The active region degree of rogueness is defined by

$$ARDoR = \delta D_{U,FS} - \delta D_{U,RS} = f_\infty e^{(t_i - t_{n+1})/\tau} (\delta D_{1,FS} - \delta D_{1,RS}). \quad (6)$$

An objection to this definition may be raised as a large AR with unusually low separation and/or tilt will yield a negligible contribution to the dipole moment ( $\delta D_U = 0$ ), yet it may be characterized by a large negative DoR value according to the proposed definition. On the other hand, this is arguably not a shortcoming of the approach: on the contrary, as the total flux emerging in a cycle of a given amplitude is more or less fixed, the emergence of a large AR with unusually low  $\delta D_U$  implies that the expected  $\delta D_U$  contribution will be “missing” at the final account, resulting in the buildup of lower-than-expected global dipole moment at the end of the cycle.

Ranking the ARs in a cycle according to their decreasing *ARDoR* values, we now set out to compare the results where *ARDoR* is explicitly considered for the top  $N$  ARs on this list, while the rest of the ARs are represented in the RS approach. We ask the question what is the lowest value for  $N$  for which the algebraic method still yields acceptable results?

### 3. *ARDoR* and rogue active regions in the $2 \times 2D$ dynamo model

Characteristics of the hybrid kinematic  $2 \times 2D$  Babcock-Leighton dynamo model developed by Lemerle et al. [2015] and Lemerle and Charbonneau [2017] are particularly suitable for a study of this type. This model couples an internal axially symmetric flux transport dynamo (FTD) with a surface flux transport (SFT) model. The FTD component module provides the new active region emergences acting as a source term in the SFT component, while the output of the SFT model is used as upper boundary condition on the FTD model. In the model, bipolar

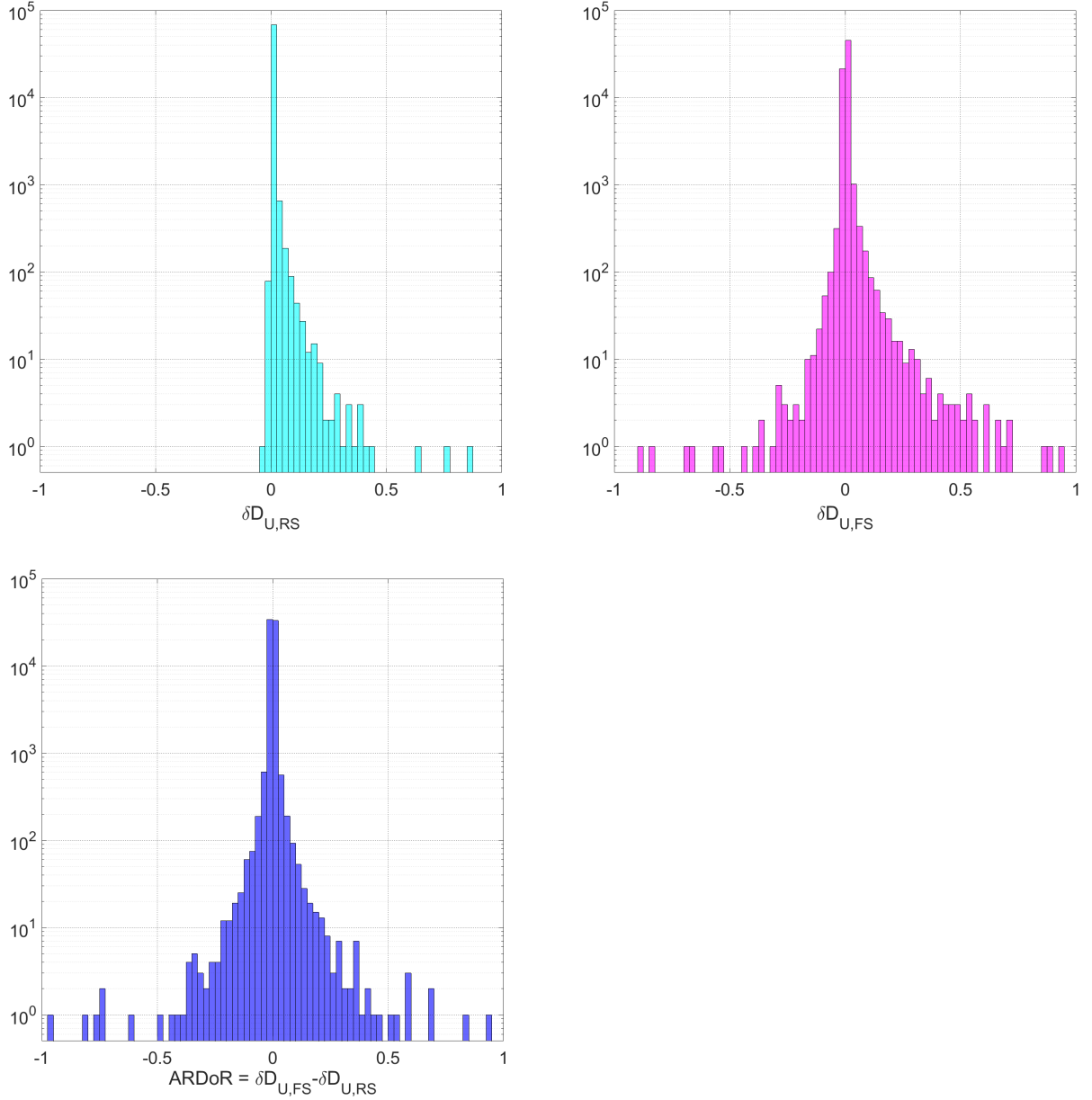


**Fig. 1.** Histograms of ultimate dipole moment contributions of individual active regions in the FS and RS cases and their differences (i.e. *ARDoR* values) measured in Gauss, based on 647 cycles with an average of 3073 active regions per cycle.

188 magnetic regions (BMRs) representing active regions are generated at the surface randomly,  
 189 with a probability based on the amplitude of the toroidal field in the deep convective zone,  
 190 their properties being drawn from a statistical ensemble constructed to obey observationally  
 191 determined statistical relationships. This makes it straightforward to extract the set of AR  
 192 properties for any cycle from the model and to convert it to a reduced stochasticity set by  
 193 setting the random fluctuations around the mean in the distributions of polarity separations

N	mean	median	st.dev.
1	0.4977	0.4565	0.4146
2	0.6184	0.6022	0.4305
3	0.6696	0.6735	0.4065
4	0.6996	0.7188	0.3953
5	0.7245	0.7490	0.3535
10	0.8139	0.8078	0.3136
20	0.8838	0.8822	0.2576
50	0.9381	0.9472	0.1917
100	0.9689	0.9816	0.1324

**Table 1.** Means, medians and standard deviations of the total ARDoR of the top  $N$  ARs divided by the total ARDoR of all ARs for cycles where the total ARDoR exceeds 15 % of the absolute change in the dipole moment  $\Delta D$  (230 cycles)

194 and tilts to zero. In addition, the numerical efficiency of the model allows to run it for a large  
 195 number of simulated solar cycles, rendering it suitable for statistical analysis of the results.

196 For the present analysis we use run results from the standard setup of the  $2 \times 2D$  model  
 197 as described in Lemerle and Charbonneau [2017]. Evaluating the parameters of the algebraic  
 198 model from the numerical results presented in Paper 1 (for the same meridional flow and  
 199 parameter values as in the dynamo model) yields  $\lambda_R = 13^\circ 6$  and  $a/\lambda_R = 3.75$ , so for the  
 200 algebraic method these values are used. The number of simulated cycles used in the analysis  
 201 was 647. The distribution of computed  $ARDoR$  values is plotted in Fig. 1.

202 ARs in each cycle are ranked by the  $ARDoR$  values. In each cycle we compute the absolute  
 203 change  $\Delta D$  in the global solar dipole moment from equation (2) for a “cocktail” of ARs,  
 204 taking the ARs with the top  $N$  highest  $ARDoR$  from the original, fully stochastic set, while  
 205 taking the rest from the RS set. For brevity, this will be referred to as the “rank- $N$   $ARDoR$   
 206 method”. The dipole moment change calculated with the rank- $N$   $ARDoR$  method is then

$$207 \quad \Delta D_{ARDoR,N} = \Delta D_{RS} + \sum_{i=1}^N ARDoR_i \quad (7)$$

208 where the AR index  $i$  is in the order of decreasing  $ARDoR$ .

209 Note that the special case  $N = 0$ , i.e. the RS set was already considered in Paper 1 where we  
 210 found that even this method yields  $\Delta D$  values in good agreement with the full simulations for  
 211 a large majority of the cycles, but the prediction breaks down for a significant minority. As we  
 212 are primarily interested in improving predictions for this minority, we first select cycles where  
 213 the difference between the  $\Delta D$  values from the fully stochastic and reduced stochasticity sets  
 214 exceeds  $\pm 15\%$ . (Note that this difference is by definition equal to the sum of  $ARDoR$ s for all  
 215 ARs in the cycle, so the condition for selection was  $(\sum_{i=1}^{N_{tot}} ARDoR_i)/\Delta D > 0.15$ , which held  
 216 for 230 cycles.)

217 Figure 2 presents histograms of the fraction of the deviation explained by ARs with the  
 218 the top  $N$  highest  $ARDoR$  values. Means, medians and standard deviations of these plots are  
 219 collected in Table 1. It is apparent that ARs with the top 10–20 highest  $ARDoR$  are sufficient

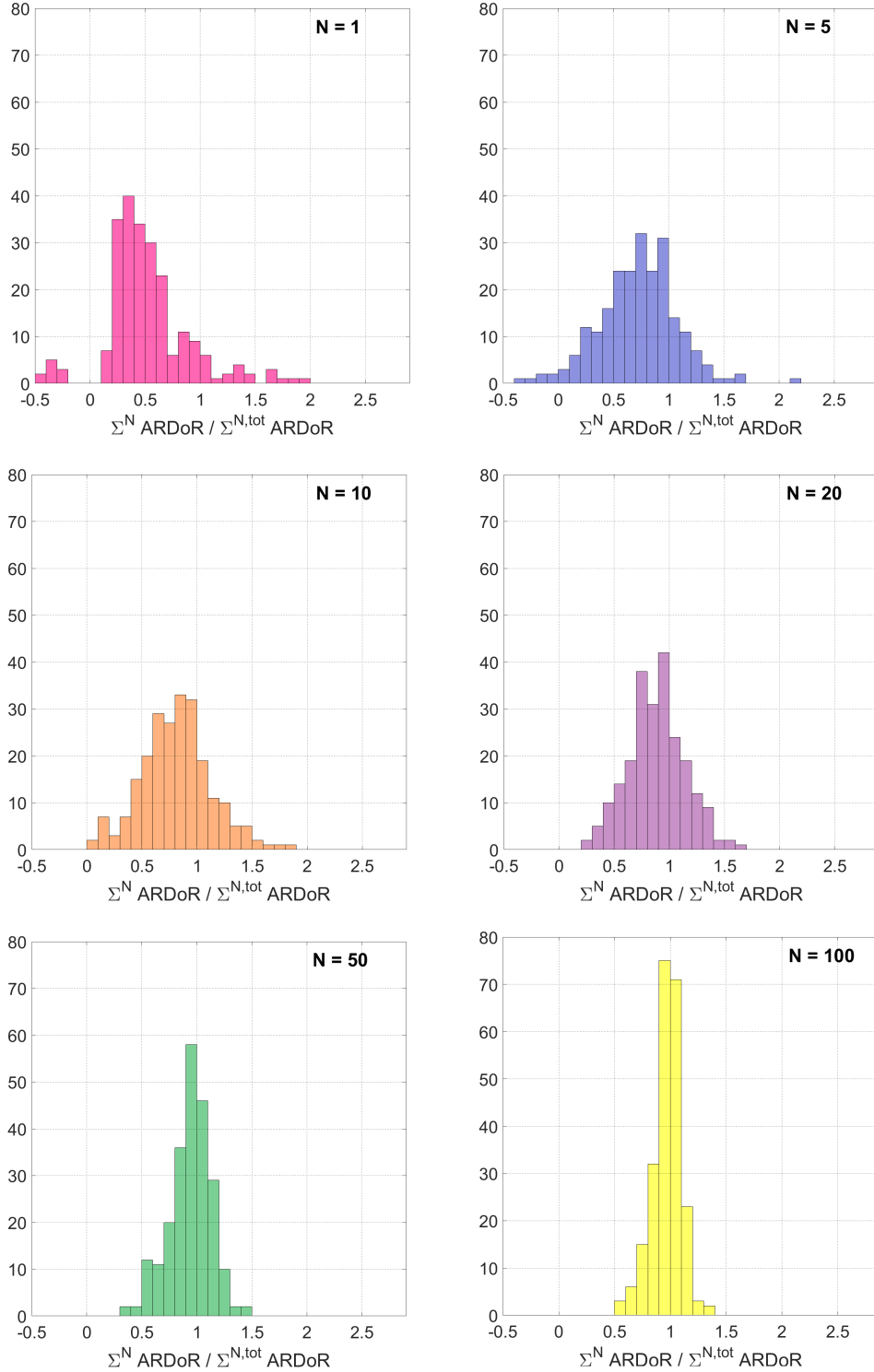


**Fig. 2.** Histograms of the total ARDoR of the top  $N$  ARs divided by the total ARDoR of all ARs for cycles where the total ARDoR exceeds 15% of the absolute change in the dipole moment  $\Delta D$  (230 cycles). The value of  $N$  is shown inside each panel.



$\Delta D_N = \Delta D_{RS} + \sum_{i=1}^N ARDoR_i$ , ranking by $ARDoR$ :				
$N$	mean	median	st.dev.	st.dev. of $(\Delta D_N - \Delta D)/\Delta D$
0	0.0578	0.0966	1.1365	0.212
5	-0.0115	0.0073	0.7360	0.128
10	-0.0330	-0.0116	0.7134	0.120
20	-0.0368	-0.0144	0.6662	0.125
50	-0.0599	-0.0406	0.6132	0.110
$N_{tot}$	-0.0499	-0.1817	0.5861	0.101

$\sum_{i=1}^N \delta D_{U,i}$ , ranking by $\delta U$ :			
$N$	mean	median	st.dev.
50	4.1280	4.1777	1.4684
100	3.1874	3.1173	1.3479
250	1.8958	1.7491	1.1311
500	1.0129	0.8471	0.9346
750	0.6003	0.4895	0.8186

**Table 2.** Means, medians and standard deviations of the residuals of various approximations relative to the simulated value of the absolute dipole moment change  $\Delta D$  during an activity cycle, as plotted in Fig. 3.

220 to explain 80–90% of the deviation of  $\Delta D$  computed with the reduced stochasticity model  
 221 from the full value of  $\Delta D$ . Even the single AR with the highest  $ARDoR$  alone can explain  
 222 50% of the deviation. Meanwhile, a significant scatter is present in the plots: e.g., adding up  
 223 the columns below 0.5 and above 1.5 in the 4th panel one finds that in  $\sim 8\%$  of these 230  
 224 deviating cycles even the rank-20  $ARDoR$  method is insufficient to reproduce the deviation  
 225 at an accuracy better than  $\pm 50\%$ . (This is  $\pm 50\%$  of the *deviation*: as in this sample the mean  
 226 deviation is roughly  $\sim 20\%$  of the expected value of  $\Delta D$ ,  $\Delta D$  itself is still reproduced with  
 227 an accuracy up to  $\pm 10\%$  for these cycles.)

228 The improvement that the  $ARDoR$  method brings to the problem of reproducing the solar  
 229 axial dipole moment at the end of a cycle is dramatically illustrated in Fig. 3. While in the  
 230 case of ranking ARs by  $\delta D$  even adding contributions from the top 750 AR yields only a  
 231 barely tolerable representation of the dipole moment variation, the  $ARDoR$  method produces  
 232 excellent agreement already for very low values of the rank  $N$ . The quality of these repre-  
 233 sentations is documented in Table 2. The standard deviation of the rank-5  $ARDoR$  method  
 234 relative to the simulation result is lower than in the case of  $\Delta D$  calculated from even the top  
 235 750 highest  $\delta D$  contributions.

236 Finally, in Fig. 4 we present histograms of the deviations from the simulated value of  $\Delta D$   
 237 computed with the various methods (FS, RS and  $ARDoR$  with different  $N$  values). Here  
 238 deviations are expressed as fractions of the actual  $\Delta D$  resulting from the simulations, i.e. the  
 239 quantities given in the headings of Table 2 are divided by  $\Delta D$ . Adding up the columns it is  
 240 straightforward to work out from this that, e.g., in the case of the rank-5  $ARDoR$  method  
 241 (i.e., considering only the top 5 highest  $ARDoR$  values and adding them to the RS algebraic  
 242 result), the deviation of  $\Delta D$  from the simulated cycle change in the global dipole moment is

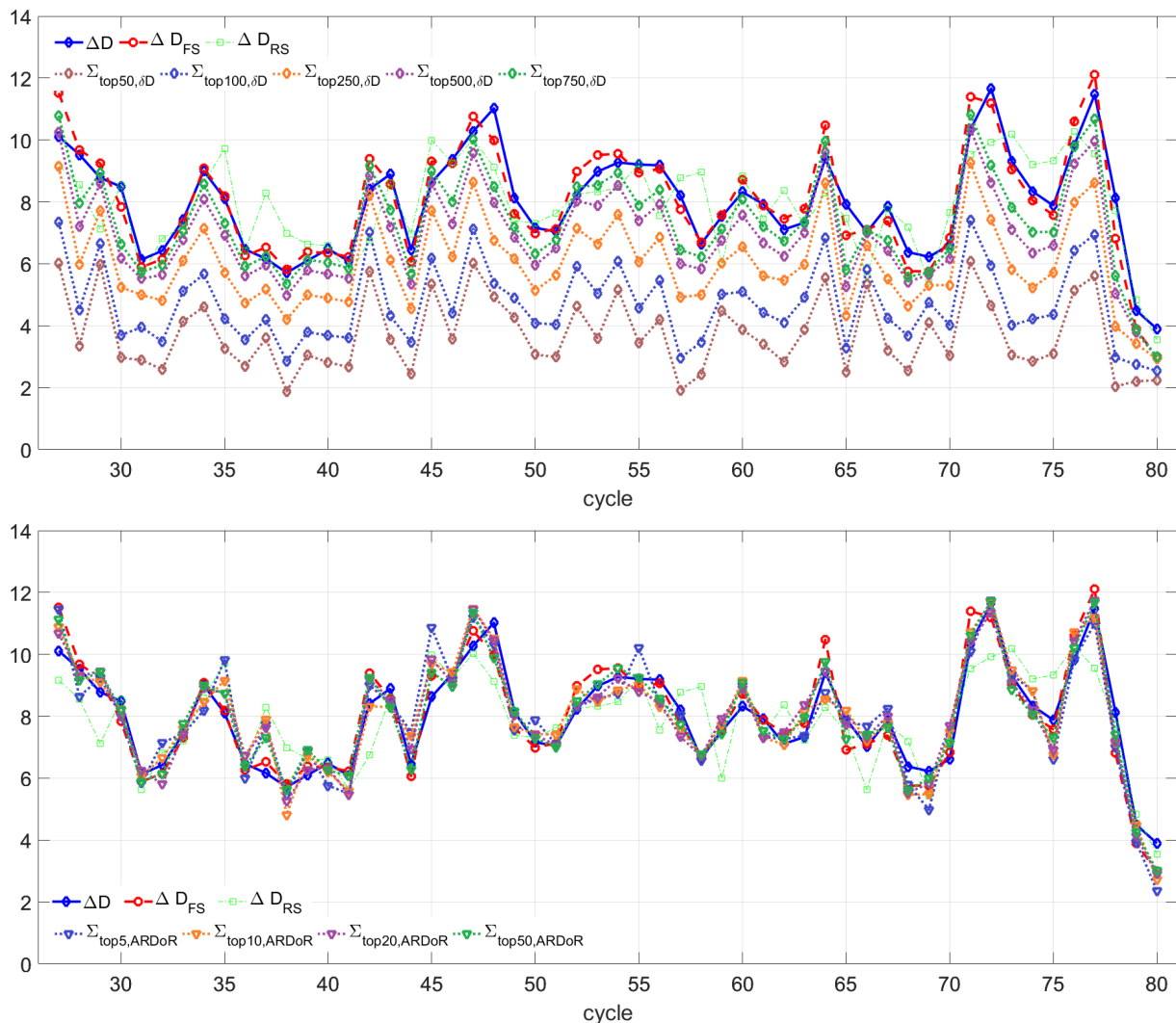


**Fig. 3.** Absolute change  $\Delta D$  on the global dipole moment during a cycle (blue solid); its approximation using the fully stochastic algebraic method (red dashed) and the reduced stochasticity algebraic method (light green dashed). The curves are compared with the absolute change computed with the algebraic method for various sets of the active regions in a cycle. *Top panel:* subsets containing ARs with the top  $N$  highest ultimate dipole contribution (FS case). *Bottom panel:* subsets containing ARs with the top  $N$  highest  $ARDoR$  values added to  $\Delta D_{RS}$ .

243 less than 15 % in 88 % of the cycles. As  $\Delta D$  is, on average, twice the amplitude of the polar  
 244 field at minimum, the rank-5  $ARDoR$  method reproduces the polar field precursor within  
 245  $\pm 30\%$  in 88 % of all cycles. This is to be compared to 74 % of the cycles in the RS case.

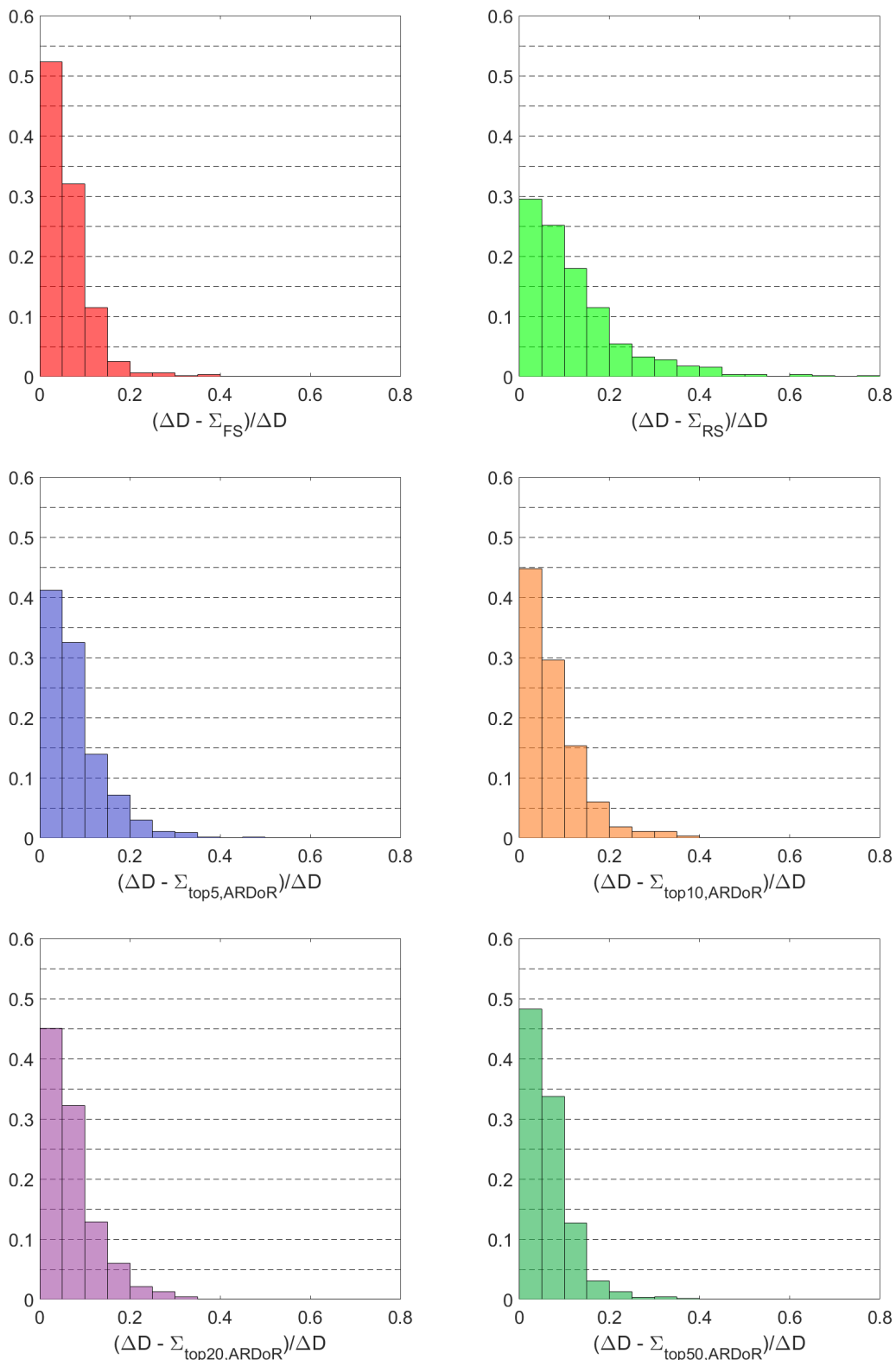


**Fig. 4.** Fractional histograms of the fractional deviation from the absolute change in dipole moment during a solar cycle, calculated summing ultimate AR contributions in the RS case + ARDoR values for ARs with the the top  $N$  highest ARDoR. ( $N = N_{\text{tot}}$  and  $N = 0$  for the first and second panels, respectively.) Colour codes are the same as in the previous plots. 11

## 4. Conclusions

In Paper 1 we introduced a method to reconstruct variations in the global axial dipole moment of the Sun by an algebraic summation of the contributions from individual active regions. In principle, for the application of this method, for each AR the optimal representation in terms of a simple bipole (or possibly several bipoles in more complex cases) needs to be known. Obtaining this information for thousands of active regions is a nontrivial task, but significant efforts have been made in this direction:

- Wang and Sheeley [1989] determined the properties of bipoles representing close to 3000 ARs with  $\Phi > 3 \cdot 10^{20}$  Mx from NSO-KP (Kitt Peak) magnetograms in Cycle 21 (1976–1986). Each AR was considered at its maximum development; recurrent ARs were multiply listed.
- Yeates et al. [2007] determined the properties of bipoles representing ARs from NSO-KP/SOLIS synoptic magnetic maps in cycles 23 and 24 (1997–2017). Each AR was considered at central meridian passage; recurrent ARs were multiply listed.
- Whitbread et al. [2018] determined initial dipole moments  $D_1$  for active regions from Kitt Peak/SOLIS synoptic magnetic maps in cycles 21–24 (1976–2017). Each AR was considered at central meridian passage; recurrent ARs were multiply listed.
- From white-light data without direct magnetic information Jiang et al. [2019] determined an indicative “dipole moment index” for sunspot groups larger than 800 MSH in cycles 21–24 (1976–2017).

Data resulting from the above listed efforts have been placed in public databases.<sup>2</sup> In addition to these, Li and Ulrich [2012] determined tilt angles for 30,600 ARs from Mt. Wilson ad MDI magnetograms in cycles 21–24 (1974–2010). Virtanen et al. [2019b] determined initial dipole moments  $D_1$  for active regions from Kitt Peak/SOLIS synoptic magnetic maps combined with SDO HMI synoptic maps in cycles 21–24 (1976–2019).

The above studies are limited to the last four cycles when magnetograms were available on a regular basis. For earlier cycles, a number of statistical analyses of sunspot data without direct magnetic information (e.g., Dasi-Espuig et al. 2010, Ivanov 2012, McClintock and Norton 2013, Baranyi 2015, Işık et al. 2018, Senthamizh Pavai et al. 2015) resulted in tilt angle values, offering some potential for use as input for models of the dipole moment evolution. Recently, information on the magnetic polarities of sunspots from Mt. Wilson measurements has been used in combination with Ca II spectroheliograms by Pevtsov et al. [2016] to construct “pseudo-magnetograms” for the period 1915–1985; the results have been benchmarked against direct observations for the last period (Virtanen et al. 2019a).

Despite these impressive efforts, the determination of AR dipole moment values to be used as input in our algebraic method is subject to many uncertainties. As discussed in the Introduction, the available data are increasingly incomplete for smaller ARs. The arbitrariness of the time chosen for the incorporation of ARs is also problematic as during their evolution the structure of ARs can change significantly due to processes not represented in the SFT models (flux emergence or localized photospheric flows). The complexities of AR structure

<sup>2</sup> VizieR and the Solar dynamo dataverse (<https://dataverse.harvard.edu/dataverse/soldynamo>), maintained by Andrés Muñoz-Jaramillo.

286 imply that their representation with a single bipole may be subject to doubt (cf. [Jiang et al.](#)  
287 [2019](#), [Iijima et al. 2019](#)). And for historical data these difficulties are further aggravated.

288 In view of these considerable difficulties, looking for ways to minimize the need for detailed  
289 input data for our algebraic method is advisable. With this objective in mind, in the present  
290 work we introduced the *ARDoR* method and tested it on a large number of activity cycles  
291 simulated with the  $2\times 2D$  dynamo model. We found that

- 292 – Including all information on the bipolar active regions appearing in a cycle, our algebraic  
293 method can reproduce the dipole moment at the end of the cycle with an error below  $\pm 30\%$   
294 in over 97% of cycles.
- 295 – Using only positions and magnetic fluxes of the ARs, and arbitrarily equating their polar-  
296 ity separations and tilts to their expected values (reduced stochasticity or RS case), the  
297 algebraic method can reproduce the dipole moment at the end of the cycle with an error  
298 below  $\pm 30\%$  in about 74% of cycles.
- 299 – Combining the RS case with detailed information on a small number  $N$  of ARs with the  
300 largest ARDoR values, the fraction of unexplained cycles is significantly reduced (from  
301 26% to 12% in the case of  $N = 5$  and a  $\pm 30\%$  accuracy threshold).

302 These results indicate that stochastic effects on the intercycle variations of solar activity  
303 are dominated by the effect of a low number of large “rogue” active regions, rather than the  
304 combined effect of numerous small ARs.

305 Beyond the academic interest of these results, the method has a potential for use in solar  
306 cycle prediction. For the realization of this potential, however, a number of further problems  
307 need to be addressed. As in forecasts the positions and fluxes of ARs are also not known,  
308 the representation of the majority of ARs not faithfully represented in our method must be  
309 stochastic also in these variables, or simply replaced by a smooth continuous distribution.  
310 Furthermore, for the selection of ARs with the top  $N$  ARDoR values these values should be  
311 theoretically be computed for all ARs. To avoid this need, “proxies” of ARDoR based on  
312 straightforward numerical criteria may need to be identified to select the ARs for which a  
313 more in-depth study is then needed to determine ARDoR values. Studies in this direction are  
314 left for further research.

315 *Acknowledgements.* This research was supported by the Hungarian National Research, Development  
316 and Innovation Fund (grant no. NKFI K-128384) and by the European Union’s Horizon 2020 research  
317 and innovation programme under grant agreement No. 739500. The collaboration of the authors was  
318 facilitated by support from the International Space Science Institute in ISSI Team 474.

## 319 References

- 320 Baranyi, T., 2015. Comparison of Debrecen and Mount Wilson/Kodaikanal sunspot group tilt  
321 angles and the Joy’s law. *Mon. Not. R. Astron. Soc.*, **447**, 1857–1865. 10.1093/mnras/stu2572,  
322 [1412.1355](#). 4
- 323 Cameron, R. H., and M. Schüssler, 2020. Loss of toroidal magnetic flux by emergence of bipolar  
324 magnetic regions. *Astron. Astrophys.*, **636**, A7. 10.1051/0004-6361/201937281, [2002.05436](#). 1

- 325 Dasi-Espuig, M., S. K. Solanki, N. A. Krivova, R. Cameron, and T. Peñuela, 2010. Sunspot group  
 326 tilt angles and the strength of the solar cycle. *Astron. Astrophys.*, **518**, A7. 10.1051/0004-  
 327 6361/201014301, [1005.1774](#). [4](#)
- 328 Işık, E., S. Işık, and B. B. Kabasakal, 2018. Sunspot group tilt angles from drawings for cycles  
 329 19-24. In D. Banerjee, J. Jiang, K. Kusano, and S. Solanki, eds., IAU Symposium, vol. 340 of  
 330 *IAU Symposium*, 133–136. 10.1017/S1743921318001461, [1804.10479](#). [4](#)
- 331 Iijima, H., H. Hotta, and S. Imada, 2019. Effect of Morphological Asymmetry between Leading  
 332 and Following Sunspots on the Prediction of Solar Cycle Activity. *Astrophys. J.*, **883**(1), 24.  
 333 10.3847/1538-4357/ab3b04, [1908.04474](#). [2](#), [4](#)
- 334 Ivanov, V. G., 2012. Joy’s law and its features according to the data of three sunspot catalogs.  
 335 *Geomagn. Aeron.*, **52**, 999–1004. 10.1134/S0016793212080130. [4](#)
- 336 Jiang, J., R. H. Cameron, and M. Schüssler, 2015. The Cause of the Weak Solar Cycle 24.  
 337 *Astrophys. J. Lett.*, **808**, L28. 10.1088/2041-8205/808/1/L28, [1507.01764](#). [1](#)
- 338 Jiang, J., Q. Song, J.-X. Wang, and T. Baranyi, 2019. Different Contributions to Space Weather and  
 339 Space Climate from Different Big Solar Active Regions. *Astrophys. J.*, **871**(1), 16. 10.3847/1538-  
 340 4357/aaf64a, [1901.00116](#). [4](#)
- 341 Lemerle, A., and P. Charbonneau, 2017. A Coupled  $2 \times 2$ D Babcock-Leighton Solar Dynamo  
 342 Model. II. Reference Dynamo Solutions. *Astrophys. J.*, **834**, 133. 10.3847/1538-4357/834/2/133,  
 343 [1606.07375](#). [3](#)
- 344 Lemerle, A., P. Charbonneau, and A. Carignan-Dugas, 2015. A Coupled  $2 \times 2$ D Babcock–Leighton  
 345 Solar Dynamo Model. I. Surface Magnetic Flux Evolution. *The Astrophysical Journal*, **810**(1),  
 346 78. 10.1088/0004-637X/810/1/78, [1511.08548](#). [2](#), [3](#)
- 347 Li, J., and R. K. Ulrich, 2012. Long-term Measurements of Sunspot Magnetic Tilt Angles.  
 348 *Astrophys. J.*, **758**(2), 115. 10.1088/0004-637X/758/2/115, [1209.1642](#). [4](#)
- 349 McClintock, B. H., and A. A. Norton, 2013. Recovering Joy’s Law as a Function of Solar Cycle,  
 350 Hemisphere, and Longitude. *Sol. Phys.*, **287**, 215–227. 10.1007/s11207-013-0338-0, [1305.3205](#). [4](#)
- 351 Nagy, M., A. Lemerle, F. Labonville, K. Petrovay, and P. Charbonneau, 2017. The Effect of “Rogue”  
 352 Active Regions on the Solar Cycle. *Sol. Phys.*, **292**, 167. 10.1007/s11207-017-1194-0, [1712.02185](#).  
 353 [1](#)
- 354 Petrovay, K., 2020. Solar cycle prediction. *Living Reviews in Solar Physics*, **17**(1), 2. 10.1007/s41116-  
 355 020-0022-z, [1907.02107](#). [2](#)
- 356 Petrovay, K., and M. Nagy, 2018. Rogue Active Regions and the Inherent Unpredictability of the  
 357 Solar Dynamo. In D. Banerjee, J. Jiang, K. Kusano, and S. Solanki, eds., IAU Symposium, vol.  
 358 340 of *IAU Symposium*, 307–312. 10.1017/S1743921318001254, [1804.03427](#). [1](#)
- 359 Petrovay, K., M. Nagy, and A. R. Yeates, 2020. Towards an algebraic method of solar cycle prediction  
 360 I. Calculating the ultimate dipole contributions of individual active regions. *Journal of Space*  
 361 *Weather and Space Climate*, **this issue**. DOI: ... . [2](#)

- 362 Pevtsov, A. A., I. Virtanen, K. Mursula, A. Tlatov, and L. Bertello, 2016. Reconstructing solar  
363 magnetic fields from historical observations. I. Renormalized Ca K spectroheliograms and pseudo-  
364 magnetograms. *Astron. Astrophys.*, **585**, A40. 10.1051/0004-6361/201526620. [4](#)
- 365 Senthamizh Pavai, V., R. Arlt, M. Dasi-Espuig, N. A. Krivova, and S. K. Solanki, 2015. Sunspot areas  
366 and tilt angles for solar cycles 7-10. *Astron. Astrophys.*, **584**, A73. 10.1051/0004-6361/201527080,  
367 [1508.07849](#). [4](#)
- 368 Tlatov, A. G., V. V. Vasil'eva, and A. A. Pevtsov, 2010. Distribution of Magnetic Bipoles on the  
369 Sun over Three Solar Cycles. *Astrophys. J.*, **717**, 357–362. 10.1088/0004-637X/717/1/357. [1](#)
- 370 Virtanen, I. O. I., I. I. Virtanen, A. A. Pevtsov, L. Bertello, A. Yeates, and K. Mursula, 2019a.  
371 Reconstructing solar magnetic fields from historical observations. IV. Testing the reconstruction  
372 method. *Astron. Astrophys.*, **627**, A11. 10.1051/0004-6361/201935606. [4](#)
- 373 Virtanen, I. O. I., I. I. Virtanen, A. A. Pevtsov, and K. Mursula, 2019b. Reconstructing solar  
374 magnetic fields from historical observations. VI. Axial dipole moments of solar active regions in  
375 cycles 21-24. *Astron. Astrophys.*, **632**, A39. 10.1051/0004-6361/201936134. [4](#)
- 376 Wang, Y. M., and J. Sheeley, N. R., 1989. Average Properties of Bipolar Magnetic Regions during  
377 Sunspot Cycle 21. *Sol. Phys.*, **124**(1), 81–100. 10.1007/BF00146521. [4](#)
- 378 Whitbread, T., A. R. Yeates, and A. Muñoz-Jaramillo, 2018. How Many Active Regions Are  
379 Necessary to Predict the Solar Dipole Moment? *Astrophys. J.*, **863**, 116. 10.3847/1538-  
380 4357/aad17e, [1807.01617](#). [1](#), [2](#), [4](#)
- 381 Yeates, A. R., D. H. Mackay, and A. A. van Ballegooijen, 2007. Modelling the Global Solar  
382 Corona: Filament Chirality Observations and Surface Simulations. *Sol. Phys.*, **245**(1), 87–107.  
383 10.1007/s11207-007-9013-7, [0707.3256](#). [4](#)